Journal of Chromatography A, 1256 (2012) 206–212

Contents lists available at SciVerse ScienceDirect

Journal of Chromatography A

journal homepage: www.elsevier.com/locate/chroma

Can slip walls improve field-flow fractionation or hydrodynamic chromatography?

G.W. Slater*, T.N. Shendruk[1]

University of Ottawa, Department of Physics, 150 Louis-Pasteur, Ottawa, ON K1N 6N5, Canada

ARTICLE INFO

Article history:
Received 14 April 2012
Received in revised form 9 July 2012
Accepted 9 July 2012
Available online 20 July 2012

Keywords:
Field-flow fractionation
Hydrodynamic chromatography
Hydrodynamic slip
Microfluidic separation
Faxén's law
Steric-Mode FFF

ABSTRACT

One way to potentially modify the performance of field-flow fractionation (FFF) would be to move the position of the maximum flow velocity away from the mid-point of the channel, for example by using walls with non-zero slip lengths. In this short communication, we extend the ideal theory of FFF to include the effects of two slip walls. Our calculations demonstrate that while the hydrodynamic chromatography limit of FFF (weak fields) is not improved by engineering devices with slip-walls, the performance of Normal-Mode FFF can be enhanced by having slip at the depletion wall in moderate fields. We also introduce a new regime, which we call Slip-Mode FFF, where a large external field (typical of Normal-Mode FFF) and a large slip at the accumulation wall lead to sharp separations characterized by an elution order that is similar to that of hydrodynamic chromatography.

1. Introduction

Field-flow fractionation (FFF) is a versatile size-separation method that has been used to analyze a wide variety of analytes including macromolecules such as starches [1] and tannins [2], microogranisms such as bacteria [3], erythroleukemia cells [4] and viral structures [5], environmental particulates [6] and nanoparticles [7]. By applying a transverse external field to a solution of sample particulates while simultaneously eluting the solution through a channel by a nonuniform, laminar flow profile, solutes elute through the device at different speeds and thus separation by size is achieved as shown schematically in Fig. 1 [8–14]. The flexibility of FFF results from the large assortment of transverse external fields that can be used. Gravitational [15,16], sedimentation [17,18], electrical [19,20], magnetic [21,22], dielectrophoretic [23,24], acoustic [25,26], photophoretic [27,28], cross-flow (both symmetrical [29,30] and asymmetrical [31,32]) and thermal [33,34] fields have all been used to generate non-uniform solute concentration distributions. The forces in both Thermal-FFF and Flow-FFF (the most widely used FFF fields) depend linearly on the particle's radius r and we will focus on this size dependence.

While interchanging external fields has been the subject of many investigations, it is generally taken for granted that the velocity of the carrier fluid obeys Poiseuille flow. Perhaps the exception to this is the difficulty associated with velocity skewing in Thermal-FFF when thermal gradients are large enough to produce viscosity gradients [35,36]. Yet, separation is completely dependent on the shape of the flow profile. In principle, it is possible to change the elution times and improve the performance of FFF over some range of particle sizes by changing the flow profile. This is what we examine in the present paper.

We will consider fractionation in an FFF channel that has arbitrary slip [37–39] at either wall. Slip is of interest to FFF because:

(i) Current Flow-FFF channels are fitted with porous ceramic frits that allow the cross-flow to enter through the depletion wall (in symmetrical Flow-FFF) and exit through the accumulation wall. Although it is well known that fluid slip can occur at porous surfaces [40–45], to the best of our knowledge, slip has not been investigated in Flow-FFF apparatuses.
(ii) Electroosmotic flow with thin Debye layers is qualitatively similar to slip flow with a Smoluchowski slip velocity [46,47]. A point-particle retention theory for the linear combination of electroosmotic flow and Poiseuille flow exists for both neutral [48] and charged [49] analytes.
(iii) The modern ability to engineer surfaces in microfluidic devices suggests that if slip is predicted to improve FFF in certain operational regimes, then channel walls can be constructed accordingly. This ability to nanoengineer patterned,

* Corresponding author.
E-mail addresses: gslater@uottawa.ca (G.W. Slater), tshen098@uottawa.ca (T.N. Shendruk).
[1] Tel.: +1 613 620 1881; fax: +1 613 562 5190.

0021-9673/$ – see front matter © 2012 Elsevier B.V. All rights reserved.
http://dx.doi.org/10.1016/j.chroma.2012.07.027

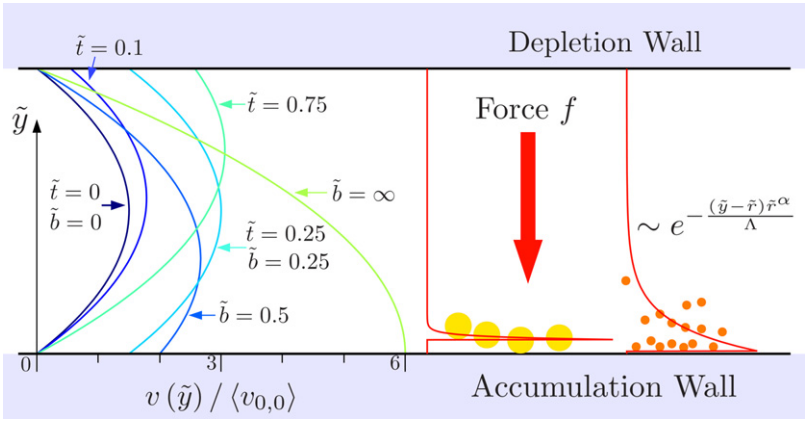

Fig. 1. Schematic of field-flow fractionation system with slip. On the left, fluid flow profiles are shown for a variety of slip lengths $\tilde{b}$ and $\tilde{t}$, for the accumulation and depletion wall respectively. Concentration distributions of large and small particles subject to a vertical external force $f(\tilde{r}) \sim \tilde{r}^{\alpha}$, where $\tilde{r}$ is the particle radius, are shown on the right. Larger particles have a sharper distribution but a larger excluded region than smaller particles.

ultrahydrophobic surfaces for drag reduction in microfluidic devices [50–56] is the primary motivation for the current theoretical study and although the source of the non-zero slip lengths is theoretically inconsequential for this study, the reader is referred to Refs. [38,57,58] as valuable reviews on superhydrophobic surfaces.

2. Theory

2.1. Carrier fluid flow profile

The flow profile $v(y)$ of a pressure driven flow between two plates separated by a distance w is parabolic with distance $\tilde{y} = y/w$ from the accumulation wall ($\tilde{}$ signifies normalization by channel height w). Slip does not change this; instead, it shifts the velocity from zero to a finite value at the walls and in doing so moves the position of the maximum from the centre of the channel. A slip length $\tilde{b}$ produces a boundary condition $v(\tilde{y}=0) = \tilde{b}(\partial v/\partial \tilde{y})\big|_{\tilde{y}=0}$ at the accumulation wall and a slip length $\tilde{t}$ makes the boundary condition at the depletion wall $v(\tilde{y}=1) = -\tilde{t}(\partial v/\partial \tilde{y})\big|_{\tilde{y}=1}$. Solving the Navier–Stokes equation, the fluid velocity profile is given by

$$v\left(\tilde{y},\tilde{b},\tilde{t}\right) = 6\langle v_{0,0}\rangle\left[-\tilde{y}^2 + \left(\frac{1+2\tilde{t}}{1+\tilde{b}+\tilde{t}}\right)\left(\tilde{y}+\tilde{b}\right)\right], \quad (1)$$

where we have stated our solution in terms of the no-slip average fluid velocity $\langle v_{0,0}\rangle = \int_0^1 v(\tilde{y},0,0)\,d\tilde{y}$ for the same pressure gradient. This equation reduces to the well-known parabolic (Poiseuille) form $v(\tilde{y},0,0) = 6\langle v_{0,0}\rangle\left[-\tilde{y}^2+\tilde{y}\right]$ in the no-slip limit. When the pressure difference is kept constant, slip moves the maximum velocity away from the centre position $\tilde{y} = 1/2$ (unless $\tilde{b} = \tilde{t}$), and increases the average flow velocity

$$\langle v\left(\tilde{b},\tilde{t}\right)\rangle = \langle v_{0,0}\rangle\left[\left(\frac{1+2\tilde{t}}{1+\tilde{b}+\tilde{t}}\right)\left(6\tilde{b}+3\right)-2\right]. \quad (2)$$

Several flow profiles are shown in Fig. 1. The equal slip such as $v(\tilde{y},0.25,0.25)$ shifts the $v(\tilde{y},0,0)$ parabolic profile up. The $v(\tilde{y},0,\infty)$ curve shows a continuous increase from zero at the no-slip wall (the depletion wall in this example) to $6\langle v_{0,0}\rangle$ at the perfect slip wall (accumulation wall).

2.2. Particle velocity

To 0th order, particles carried by the flow move at the same speed as the solvent at the centre of mass of the particle, $v\left(\tilde{y},\tilde{b},\tilde{t}\right)$, but to correct for the curvature of the fluid profile over the surface of a spherical particle of finite radius $\tilde{r}$, Faxén's law must be applied. The ideal velocity of the solute particle is then found to be given by

$$\mathcal{V}\left(\tilde{r},\tilde{y},\tilde{b},\tilde{t}\right) = \left[1+\frac{\tilde{r}^2}{6}\nabla^2\right]\; v\left(\tilde{y},\tilde{b},\tilde{t}\right) = v\left(\tilde{y},\tilde{b},\tilde{t}\right) - 2\tilde{r}^2\langle v_{0,0}\rangle. \quad (3)$$

The retention theory used here is called "ideal" primarily because it neglects hydrodynamic interactions between the solute particles and the walls (although other complications such as concentration effects [59], *etc.* [60] are also assumed insignificant). Hydrodynamic interactions can generally be divided into inertial lift forces, which act perpendicular to the channel walls, and drag forces, which act anti-parallel to the direction of flow. The lift forces generally have components both towards (due to the shear-gradient) and also away from (due to symmetry breaking by the wall) the walls, which establish an equilibrium height [61]. Lift forces can be kept small by keeping the particle Reynolds number well below unity or be utilized to separate particles by inertial focusing [62–64] or Hyperlayer-Mode FFF [65,16]. The increased drag arises because the no-slip conditions on both the surface of the mobile particles and on the channel walls cause greater shearing of the fluid and so generate a greater effective friction coefficient than the same particulates would have in free solution, which reduces $\mathcal{V}$ from the value predicted by Eq. (3) [66]. This effect may become significant as the particle size approaches the channel height and so the ideal theory presented here would tend to overpredict the retention ratio (although this effect is reduced by large slip lengths [51]).

2.3. Concentration distribution

In FFF, solute particles are pushed against the accumulation wall (Fig. 1) by a force $f(\tilde{r}) \sim \tilde{r}^{\alpha}$ but are dispersed by diffusion. The competition between potential and thermal energy is described by the retention parameter $\lambda = k_B T/fw = \Lambda \tilde{r}^{-\alpha}$ and leads to an exponential concentration distribution

$$c(\tilde{y}) \sim \begin{cases} e^{-(\tilde{y}-\tilde{r})\tilde{r}^{\alpha}/\Lambda} & \text{for } \tilde{r} < \tilde{y} < 1-\tilde{r} \\ 0 & \text{otherwise.} \end{cases} \quad (4)$$

The dimensionless *device retention parameter* Λ describes the FFF apparatus without implicit reference to particle size [67]. As stated earlier, because of its connection to Flow-FFF we will focus on $\alpha = 1$ (linear scaling) unless otherwise noted. Different sized solute particles have different concentration distributions dictated by their relevant Boltzmann factor and so sample the fluid velocity profile differently (Fig. 1).